# A Noble-Metal-Free Hydrogen Evolution Catalyst Grafted to Visible Light-Absorbing Semiconductors

**ARTICLE** *in* JOURNAL OF PHYSICAL CHEMISTRY LETTERS · JANUARY 2013

Impact Factor: 7.46 · DOI: 10.1021/jz400028z



**2 AUTHORS**, INCLUDING:

Gary F Moore
Arizona State University
**46** PUBLICATIONS **693** CITATIONS

SEE PROFILE

THE JOURNAL OF PHYSICAL CHEMISTRY Letters

Letter

pubs.acs.org/JPCL

# A Noble-Metal-Free Hydrogen Evolution Catalyst Grafted to Visible Light-Absorbing Semiconductors

Gary F. Moore* and Ian D. Sharp*

Joint Center for Artificial Photosynthesis (JCAP), Lawrence Berkeley National Laboratory, Berkeley, California 94720, United States

Supporting Information

**ABSTRACT:** We report a method for facile connection of a nickel bisdiphosphine-based functional mimic of the active site of hydrogenase to photocathodes that are relevant to artificial photosynthesis. This procedure exploits the UV-induced immobilization chemistry of alkenes to gallium phosphide and silicon surfaces. The photochemical grafting provides a means for patterning molecular linkers with attachment points to catalysts. Successful grafting is characterized by grazing angle attenuated total reflection Fourier transform infrared spectroscopy (GATR-FTIR), which shows catalyst vibrational modes, as well as X-ray photoelectron spectroscopy (XPS), which confirms the presence of intact Ni complex on the surface. The modular nature of this approach allows independent modification of the light absorber, bridging material, anchoring functionality, or catalyst as new materials and discoveries emerge.

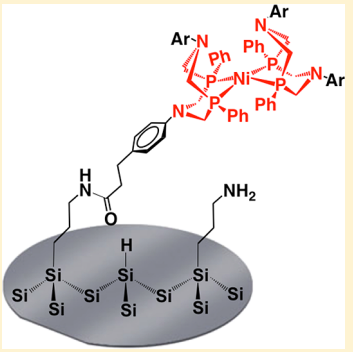


**SECTION:** Surfaces, Interfaces, Porous Materials, and Catalysis

Solar energy offers a desirable approach to fulfilling global human energy demands with minimal environmental impact,[1] provided efficient, low-cost systems can be developed for its capture, conversion, and storage. In biology, solar energy is collected by the process of photosynthesis and is ultimately stored in chemical bonds via enzyme catalysis.[2−4] Avoiding the use of rare-earth metals, high temperatures, and extreme pH, enzymes provide appropriate three-dimensional environments for binding substrate and lowering transition-state energies along a reaction coordinate. Thus, they have exceptionally high activities, yet are limited by their size, fragility, and scalability for applications in many industrial and technological processes. In this context, the development of advanced materials and techniques for manipulating matter on the nanoscale has allowed significant advances toward mimicking favorable aspects of the chemistry of biological systems into human-engineered constructs while excluding features that are undesirable.[5−11]

An elegant example of such mimicry is captured in the bioinspired nickel catalysts reported by DuBois and co-workers.[12−14] In these complexes, bisdiphosphines provide a soft ligand environment that stabilizes the formation of low-valent nickel during the catalytic cycle, and pendent amine bases provide proton relays that deliver substrate to a metal hydride, facilitating the formation of hydrogen via a low-energy pathway. Le Goff et al. have reported an analogous nickel-based molecular catalyst **2**$(BF_4)_2$ (Chart 1) bearing activated esters in the para position of the nitrogen-bound phenyl groups of the 1,3,5,7-tetraphenyl-1,5-diaza-3,7-diphosphacyclooctane ligand for immobilization onto amine-modified carbon nanotubes (CNTs) via formation of stable covalent amide linkages.[15,16] The electrocatalytic material allows sustained performance for

**Chart 1. Compounds 1 and 2**

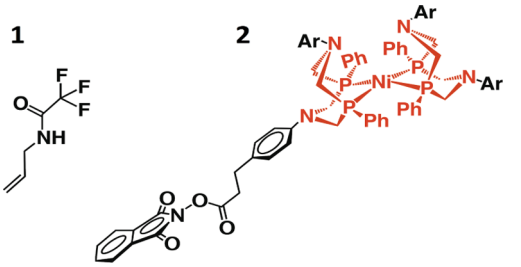


the production (TON > 100 000) and oxidation (TON > 35 000) of hydrogen, as well as operation under acidic aqueous conditions (0.5 M $H_2SO_4$). Although this represents significant advancement from previous work conducted in organic solvents using organic acids as a proton source, significant challenges to closing the solar-to-fuels loop remain.

Attachment of molecular sensitizers and catalysts to wide band gap semiconductors has been pursued in developing integrated photoanodes and more recently photocathodes.[17−25] Herein, we report a method for covalently attaching **2**$(BF_4)_2$ to visible light-absorbing semiconductors including *p*-type (100) GaP ($E_g$ = 2.26 eV) and *p*-type (111) Si ($E_g$ = 1.12 eV). The band gap of the latter is nearly optimal for harvesting solar energy in a tandem device configuration as a photocathode (Figure S1), while the conduction bands of both materials are poised negative of the $H^+/H_2$ redox couple.[26−29] Thus, these

**Received:** January 6, 2013
**Accepted:** January 25, 2013

   dx.doi.org/10.1021/jz400028z | *J. Phys. Chem. Lett.* 2013, 4, 568−572

materials are relevant to light capture and conversion applications in artificial photosynthesis.[30−35]

Our grafting procedure exploits the UV-induced immobilization chemistry of alkenes to GaP and Si surfaces (see Supporting Information (SI) for experimental details).[36−40] As a starting point, we use *N*-allyl-2,2,2-trifluoro-acetamide (**1**) to photochemically attach masked amines onto semiconductor surfaces. The terminal trifluoroacetamide head groups are then chemically removed under acidic conditions yielding an amine modified semiconductor surface. Catalyst attachment is achieved by treatment of the modified surface with a solution containing $\mathbf{2}(BF_4)_2$ (see SI).

Grazing angle attenuated total reflection Fourier transform infrared spectroscopy (GATR-FTIR) and X-ray photoelectron spectroscopy (XPS) are used to characterize successful chemical modification of the surface following each stage of wet-chemical processing. To remove surface oxide layers and provide a foundation for photochemical grafting of **1**, degreased (111) Si and (100) GaP surfaces were treated in buffered hydrofluoric acid (BHF). FTIR of (111) Si indicates monohydride termination of the surface (Figure S8), and XPS confirms complete removal of the oxide (Figure S9). By contrast, (100) GaP is characterized by significant residual surface oxygen coverage. Although the present measurements do not allow determination of the specific identities of surface oxygen moieties on GaP, static water contact angles of <10° suggest a dominant coverage by hydrophilic hydroxyl groups. Thus, comparison of hydrogen-terminated (111) Si to oxygen-terminated (100) GaP provides a means to test the broad applicability of this attachment strategy to different semiconductor surfaces.

Figures 1a and 2a show GATR-FTIR spectra of (100) GaP and (111) Si, respectively, including spectra collected following

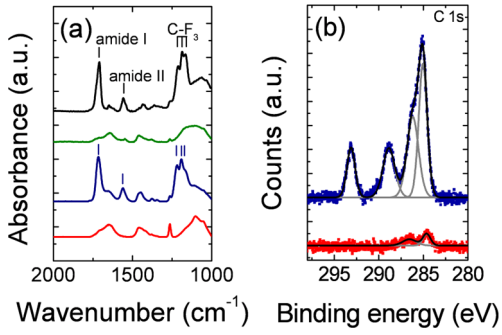


**Figure 1.** (a) GATR-FTIR spectra of (100) GaP following BHF treatment (red line), UV photochemical reaction with **1** (blue line), and chemical deprotection (green line) as well as an FTIR spectrum of **1** in KBr (black line). (b) XPS of the C 1s region of BHF-treated (100) GaP before (red squares) and after (blue squares) reaction with **1**. Solid lines are component (gray) and overall (black) fits to the experimental data.

photochemical grafting of **1**, and after chemical removal of the trifluoroacetamide protecting group. A FTIR spectrum of neat **1** in KBr is shown for comparison. Characteristic vibrational modes of the linker, including the amide I band at 1715 $cm^{-1}$, the amide II band at 1560 $cm^{-1}$, and the C−F stretches from the $CF_3$ protecting group at 1211, 1186, and 1165 $cm^{-1}$,[41] are observed on the functionalized GaP and Si surface. Following chemical deprotection, near complete disappearance of these bands is observed on GaP. For the case of Si, a vibrational band

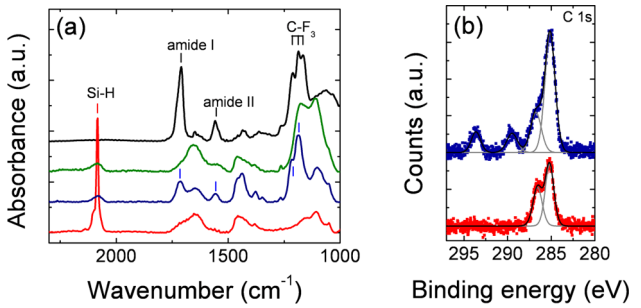


**Figure 2.** (a) GATR-FTIR spectra of (111) Si following BHF treatment (red line), UV photochemical reaction with **1** (blue line), and chemical deprotection (green line) as well as an FTIR spectrum of neat **1** in KBr (black line). (b) XPS of the C 1s region of BHF-treated (111) Si before (red squares) and after (blue squares) reaction with **1**. Solid lines are component (gray line) and overall (black line) fits to the experimental data.

associated with the formation of Si−O bonds at non-functionalized surface sites conceals the C−F stretch region; however, XPS of the C 1s and F 1s regions confirms chemical deprotection. We note that the presence of adsorbed atmospheric water masks the N−H stretch region and precludes analysis of the primary amine group following deprotection.

Figures 1b and 2b show XPS C 1s core level spectra of (100) GaP and (111) Si, respectively, including spectra collected before and after functionalization with **1**. The dominant peak, centered at 284.8 eV, is assigned to C atoms in the short aliphatic chain of the linker, along with a partial contribution from adventitious carbon. The shoulder at 286.1 eV is attributed to C atoms in grafted molecules bound to N, as well as C bound to O in adventitious carbon. The spectral components at 293.0 and 288.9 eV are unambiguously assigned to C atoms in the $CF_3$ and C═O groups of the grafted molecules, respectively.

UV photochemical grafting of olefins to H-terminated surfaces is well established and results in direct Si−C bonds.[38−40] Recently, this method has been extended to functionalization of hydroxylated surfaces. While the mechanistic details of this reaction are not settled, molecular binding appears to occur over a bridging oxygen atom (e.g., Ti−O−C on $TiO_2$).[41−44] For the case of (100) GaP investigated here, inspection of the substrate XPS core level spectra provides direct evidence for molecular bonding over an oxygen bridge. In particular, the Ga $2p_{3/2}$ spectral intensity ratio, $A_{Ga-O}/A_{Ga-P}$, is 0.13 both before and after molecular attachment, despite significant attenuation of the substrate signal due to the presence of the grafted molecular layer. Likewise, the P 2p spectral intensity ratio, $A_{P-O}/A_{P-Ga}$, is unaffected by photochemical functionalization, indicating that molecular bonding is not accompanied by loss of oxygen from the surface. We conclude that in contrast to Si, on which direct Si−C bonds form between the semiconductor and molecular layer, grafting on GaP likely occurs over bridging oxygen atoms.

Figure 3 shows GATR-FTIR spectra of *p*-type GaP and Si surfaces following the catalyst immobilization procedure via reaction of $\mathbf{2}(BF_4)_2$ with the primary amines of the molecular linkers grafted on the semiconductor substrates. For comparison, FTIR spectra of the unbound catalyst in KBr are included. In the carbonyl stretch region of all spectra, three distinct peaks, located at 1816, 1785, and 1742 $cm^{-1}$, are observed. These are


dx.doi.org/10.1021/jz400028z | J. Phys. Chem. Lett. 2013, 4, 568−572

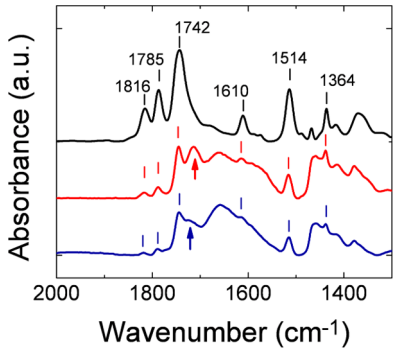


**Figure 3.** GATR-FTIR spectra of $2(BF_4)_2$ grafted to (100) GaP (blue line) and $2(BF_4)_2$ grafted to Si (red line) as well as an FTIR spectrum of $2(BF_4)_2$ in KBr. Arrows mark the carbonyl stretch (1715 $cm^{-1}$) associated with attachment of $2(BF_4)$ to the amine-terminated GaP and Si surfaces.

assigned to the symmetric and antisymmetric stretching modes of the pthalimide imide groups, as well as the carbonyl of the ester bond to the pthalimide. The presence of these modes after catalyst attachment indicates that a fraction of unreacted pthalimde groups are present on both the GaP and Si surfaces. However, an additional feature, at 1715 $cm^{-1}$ (marked with an arrow in Figure 2), is present only for the Si and GaP samples treated with $2(BF_4)_2$ and is not observed for the unreacted catalyst. This new feature is consistent with partial deprotection of the activated esters on $2(BF_4)_2$ during the immobilization yielding carboxylic acids (Figure S6). Additional vibrational modes, at 1610 and 1514 $cm^{-1}$ ($\nu(C{=}C)_{aromatic}$) and 1364 $cm^{-1}$ (C−N stretch) are present in both the reference spectrum of $2(BF_4)_2$ in KBr and in spectra obtained after reaction with amine-terminated substrates, providing additional evidence for the presence of $2(BF_4)_2$ after immobilization on both Si and GaP.

Although GATR-FTIR enables investigation of the vibrational modes of the ligand structure, modes arising from the Ni core are not spectroscopically accessible using our current instrument configuration (see SI). However, the presence of the intact nickel complex on both Si and GaP surfaces is confirmed by XPS. Survey spectra show the presence of C, N, O, and Ni elements of the catalyst, as well as F of the $BF_4^-$ counterion (see Figure S10). Furthermore, the Ni 2p core level region spectra (Figure 4) shows peaks centered at 856.0 eV ($2p_{3/2}$) and 873.5 eV ($2p_{1/2}$), that are characteristic of a $Ni^{II}$ oxidation state and are consistent with previous reports of immobilized $2(BF_4)_2$ catalyst on carbon-based materials.[15] Yet, we note that the observed shakeup satellite features in the Ni 2p region, which are present in Figure 4, as well as in previous reports of $2(BF_4)_2$ immobilization on CNT networks,[15] are found only in paramagnetic species,[45] indicating some structural distortion, as compared to the unbound diamagnetic $Ni^{II}$ complex. Nevertheless, it has been shown that, despite apparent structural changes, immobilized $2(BF_4)_2$ retains electrocatalytic activity on carbon based materials.[15] A detailed investigation of these changes in structure and catalytic activity on our surface modified semiconductors is currently underway.

In summary, surface sensitive spectroscopic methods verify our synthetic efforts dedicated to construction of hybrid composite materials that structurally interface a hydrogen evolution catalyst to visible light-absorbing semiconductors. Passivation of the underlying semiconductor surface is not addressed in this work. Generation of surface defects, oxides,

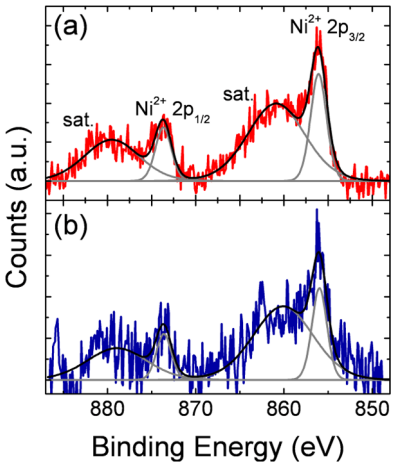


**Figure 4.** Ni 2p core level XPS spectra of (a) $2(BF_4)_2$ grafted to (111) Si (red line) and (b) $2(BF_4)_2$ grafted to (100) GaP (blue line). The solid gray and solid black lines are the component and overall fits, respectively.

and trap states resulting from incomplete surface coverage will degrade the photoelectrochemial properties of the semiconductor.[40] However, strategies such as the use of mixed monolayers that incorporate surface-methyl terminating groups[46,47] or the use of atomic layer-deposited tunnel oxides[48−50] already offer promising approaches to surface stabilization and are compatible with the approach reported here. Although a number of scientific challenges remain, this work represents an important step toward developing an integrated photocathode material for use in a tandem solar-fuels generator. Further, the modular nature of this approach allows independent modification of the light absorber, bridging material, anchoring functionality, or catalyst as new materials and discoveries emerge. This approach could allow catalysts made from earth-abundant elements, tethered over structured photocathodes,[31,32,49] to replace the use of precious metal catalysts.

## ■ ASSOCIATED CONTENT

### Supporting Information

Materials, instruments, synthesis, UV−vis−NIR spectra, XPS spectra, GATR-FTIR spectra, cyclic voltammetry. This material is available free of charge via the Internet at http://pubs.acs.org.

## ■ AUTHOR INFORMATION

### Corresponding Author

*E-mail: gfmoore@lbl.gov (G.F.M.); idsharp@lbl.gov (I.D.S.).

### Author Contributions

The manuscript was written through contributions of all authors. All authors have given approval to the final version of the manuscript.

### Notes

The authors declare no competing financial interest.

## ■ ACKNOWLEDGMENTS

This material is based upon work performed by the Joint Center for Artificial Photosynthesis, a DOE Energy Innovation Hub, supported through the Office of Science of the U.S. Department of Energy under Award Number DE-SC0004993.

## REFERENCES


(1) Lewis, N. S.; Nocera, D. J. Powering the Planet: Chemical Challenges in Solar Energy Utilization. *Proc. Natl. Acad. Sci.U.S.A.* **2006**, *103*, 15729−15735.

(2) Hirst, J.; Armstrong, F. A. Reversibility and Efficiency in Electrocatalytic Energy Conversion and Lessons from Enzymes. *Proc. Natl. Acad. Sci. U.S.A.* **2011**, *108*, 14049−14054.

(3) McEvoy, J. P.; Brudvig, G. W. Water-Splitting Chemistry of Photosystem II. *Chem. Rev.* **2006**, *106*, 4455−4483.

(4) Albery, W. J.; Knowles, J. R. Evolution of Enzyme Function and the Development of Catalytic Efficiency. *Biochemistry* **1976**, *15*, 5631−5640.

(5) Moore, G. F.; Brudvig, G. W. Energy Conversion in Photosynthesis: A Paradigm for Solar Fuel Production. *Annu. Rev. Condens. Matter Phys.* **2011**, *2*, 303−327.

(6) Walter, M. G.; Warren, E. L.; Mckone, J. R.; Boettcher, S. W.; Mi, Q.; Santori, E. A.; Lewis, N. S. Solar Water Splitting Cells. *Chem. Rev.* **2010**, *110*, 6446−6473.

(7) Hambourger, M. F.; Moore, G. F.; Kramer, D. M.; Gust, D.; Moore, A. L; Moore, T. A. Biology and Technology for Photochemical Fuel Production. *Chem. Soc. Rev.* **2009**, *38*, 25−35.

(8) Najafpour, M. M.; Moghaddam, A. N.; Allakhverdiev, S. I. Govindjee Biological Water Oxidation: Lessons from Nature. *Biochim. Biophys. Acta* **2012**, *8*, 1110−1121.

(9) Barber, J. Photosynthetic Energy Conversion: Natural and Artificial. *Chem. Soc. Rev.* **2009**, *38*, 185−196.

(10) Lubitz, W.; Reijerse, E. J.; Messinger, J. Solar Water-Splitting into $H_2$ and $O_2$: Design Principles of Photosystem II and Hydrogenases. *Energy Environ. Sci.* **2008**, *1*, 15−31.

(11) Wasielewski, M. R. Photoinduced Electron Transfer in Supramolecular Systems for Artificial Photosynthesis. *Chem. Rev.* **1992**, *92*, 435−461.

(12) Wilson, A. D.; Newell, H. N.; McNevin, M. J.; Muckerman, J. T.; DuBois, M. R.; DuBois, D. L. Hydrogen Oxidation and Production Using Nickel-Based Molecular Catalysts with Positioned Proton Relays. *J. Am. Chem. Soc.* **2006**, *358*, 5861−5872.

(13) Kilgore, U. J.; Roberts, J. A. S.; Pool, D. H.; Appel, A. M.; Stewart, M. P.; DuBois, M. R.; Dougherty, W. G.; Kassel, W. S.; Bullock, R. M.; DuBois, D. L. $[Ni(P^{Ph}{}_2N^{C6H4X}{}_2)_2]^{2+}$ Complexes as Electrocatalysts for $H_2$ Production: Effect of Substituents, Acids, and Water on Catalytic Rates. *J. Am. Chem. Soc.* **2011**, *133*, 5861−5872.

(14) Helm, M. L.; Stewart, M. P.; Bullock, R. M.; DuBois, M. R.; DuBois, D. L. A Synthetic Nickel Electrocatalyst with a Turnover Frequency Above 100,000 $s^{-1}$ for $H_2$ Production. *Science* **2011**, *333*, 863−866.

(15) Le Goff, A.; Artero, V.; Jousselme, B.; Tran, P. D.; Guillet, N.; Metaye, R.; Fihri, A.; Palacin, S.; Fontecove, M. From Hydrogenases to Noble Metal-Free Catalytic Nanomaterials for $H_2$ Production and Uptake. *Science* **2009**, *326*, 1384−1387.

(16) Hambourger, M. H.; Moore, T. A. Nailing Down Nickel for Electrocatalysis. *Science* **2009**, *326*, 1355−1356.

(17) Youngblood, W. J.; Lee, S.-H. A.; Kobayashi, Y.; Hernandez-Pagan, E. A.; Hoertz, P. G.; Moore, T. A.; Moore, A. L.; Gust, D.; Mallouk, T. E. Photoassisted Overall Water Splitting in a Visible Light-Absorbing Dye-Sensitized Photoelectrochemical Cell. *J. Am. Chem. Soc.* **2009**, *131*, 926−927.

(18) Brimblecombe, R.; Koo, A.; Dismukes, G. C.; Swiegers, G. F.; Spiccia, L. Solar Driven Water Oxidation by a Bioinspired Manganese Molecular Catalyst. *J. Am. Chem. Soc.* **2010**, *132*, 2892−2894.

(19) Li, L.; Duan, L.; Xu, Y.; Gorlov, M.; Hagfeldt, A.; Sun, L. A Photoelectrochemical Device for Visible Light Driven Water Splitting by a Molecular Ruthenium Catalyst Assembled on Dye-Sensitized Nanostructured $TiO_2$. *Chem. Commun.* **2010**, *46* (39), 7307−7309.

(20) Li, G.; Sproviero, E. M.; McNamara, W. R.; Snoeberger, R. C.; Crabtree, R. H.; Brudvig, G. W.; Batista, V. S. Reversible Visible-Light Photooxidation of an Oxomanganese Water Oxidation Catalyst Covalently Anchored to $TiO_2$ Nanoparticles. *J. Phys. Chem. B* **2010**, *114*, 14214−14222.

(21) Moore, G. F.; Blakemore, J. D.; Milot, R. L.; Hull, J. F.; Song, H.-e.; Cai, L.; Schmuttenmaer, C. A.; Crabtree, R. H.; Brudvig, G. W. A Visible Light Water-Splitting Cell with a Photoanode Formed by Codeposition of a High-Potential Porphyrin and an Iridium Water-Oxidation Catalyst. *Energy Environ. Sci.* **2011**, *4*, 2389−2392.

(22) Lakadamyali, F.; Reisner, E. Photocatalytic $H_2$ Evolution from Neutral Water with a Molecular Cobalt Catalyst on a Dye-Sensitised $TiO_2$ Nanoparticle. *Chem. Commun.* **2011**, *47*, 1695−1697.

(23) Song, W.; Glasson, C. R. K.; Luo, H.; Hanson, K.; Brennaman, M. K.; Concepcion, J. J.; Meyer, T. J. Photoinduced Stepwise Oxidative Activation of a Chromophore Catalyst Assembly on $TiO_2$. *J. Phys. Chem. Lett.* **2011**, *2*, 1808−1813.

(24) Zhao, Y.; Swierk, J. R.; Megiatto, J. D.; Sherman, B. D.; Youngblood, J. W.; Qin, D.; Lentza, D. M.; Moore, A. L.; Moore, T. A.; Gust, D.; et al. Improving the Efficiency of Water Splitting in Dye-Sensitized Solar Cells by Using a Biomimetic Electron Transfer Mediator. *Proc. Natl. Acad. Sci. U.S.A.* **2012**, *109*, 15612−15616.

(25) Gardner, J. M.; Beyler, M.; Karnahl, M.; Tschierlei, S.; Ott, S.; Hammarström, L. Light-Driven Electron Transfer between a Photosensitizer and a Proton-Reducing Catalyst Co-adsorbed to NiO. *J. Am. Chem. Soc.* **2012**, *134*, 19322−19325.

(26) Hanna, M. C.; Nozik, A. J. Solar Conversion Efficiency of Photovoltaic and Photoelectrolysis Cells with Carrier Multiplication Absorbers. *J. Appl. Phys.* **2006**, *100*, 074510−1−074510−8.

(27) Grätzel, M. Photoelectrochemical Cells. *Nature* **2001**, *414*, 338−344.

(28) Blankenship, R. E.; Tiede, D. M.; Barber, J.; Brudvig, G. W.; Fleming, G.; Ghirardi, M.; Gunner, M. R.; Junge, W.; Kramer, D. M.; Melis, A.; et al. Comparing Photosynthetic and Photovoltaic Efficiencies and Recognizing the Potential for Improvement. *Science* **2011**, *332*, 805−809.

(29) Hammarström, L.; Winkler, J. R.; Gray, H. B.; Styring, S. Shedding Light on Solar Fuel Efficiencies. *Science* **2011**, *333*, 288.

(30) Reece, S. Y.; Hamel, J. A.; Sung, K.; Jarvi, T. D.; Esswein, A. J.; Pijpers, J. J. H.; Nocera, D. G. Wireless Solar Water Splitting Using Silicon-Based Semiconductors and Earth-Abundant Catalysts. *Science* **2012**, *334*, 645−648.

(31) Sun, J.; Liu, C.; Yang, P. Surfactant-Free, Large-Scale, Solution−Liquid−Solid Growth of Gallium Phosphide Nanowires and Their Use for Visible-Light-Driven Hydrogen Production from Water Reduction. *J. Am. Chem. Soc.* **2011**, *133*, 19306−19309.

(32) Boettcher, S. W.; Warren, E. L.; Putnam, M. C.; Santori, E. A.; Turner-Evans, D.; Kelzenberg, M. D.; Walter, M. G.; McKone, J. R.; Brunschwig, B. S.; Atwater, H. A.; et al. Photoelectrochemical Hydrogen Evolution Using Si Microwire Arrays. *J. Am. Chem. Soc.* **2011**, *133*, 1216−1219.

(33) Hou, Y.; Abrams, B. L.; Vesborg, P. C. K.; Björketun, M. E.; Herbst, K.; Bech, L.; Setti, A. M.; Damsgaard, C. D.; Pedersen, T.; Hansen, O.; et al. Bioinspired Molecular Co-Catalysts Bonded to a Silicon Photocathode for Solar Hydrogen Evolution. *Nat. Mater.* **2011**, *10*, 434−438.

(34) Kumar, B.; Smieja, J. M.; Kubiak, C. P. Photoreduction of $CO_2$ on p-Type Silicon Using $Re(bipy\text{-}But)(CO)_3Cl$: Photovoltages Exceeding 600 mV for the Selective Reduction of $CO_2$ to CO. *J. Phys. Chem. C* **2010**, *114*, 14220−14223.

(35) Barton, E. E.; Rampulla, D. M.; Bocarsly, A. B. Selective Solar-Driven Reduction of $CO_2$ to Methanol Using a Catalyzed p-GaP Based Photoelectrochemical Cell. *J. Am. Chem. Soc.* **2008**, *130*, 6342−6344.

(36) Wang, X.; Ruther, R. E.; Streifer, A. J.; Hamers, R. J. UV-Induced Grafting of Alkenes to Silicon Surfaces: Photoemission versus Excitons. *J. Am. Chem. Soc.* **2010**, *132*, 4048−4049.

(37) Richards, D.; Zemlyanov, D.; Ivanisevic, A. Assessment of the Passivation Capabilities of Two Different Covalent Chemical Modifications on GaP(100). *Langmuir* **2010**, *18*, 10676−10684.

(38) Cicero, R. L.; Linford, M. R.; Chidsey, C. E. D. Photoreactivity of Unsaturated Compounds with Hydrogen-Terminated Silicon (111). *Langmuir* **2000**, *16*, 5688−5695.

(39) Terry, J.; Linford, M. R.; Wigren, C.; Cao, R. Y.; Pianetta, P.; Chidsey, C. E. D. Alkyl-Terminated Si(111) Surfaces: A High-

resolution, Core Level Photoelectron Spectroscopy Study. *J. Appl. Phys.* **1999**, *85*, 213−221.
(40) Buriak, J. M. Organometallic Chemistry on Silicon and Germanium Surfaces. *Chem. Rev.* **2002**, *102*, 1271−1308.
(41) Li, B.; Franking, R.; Landis, E. C.; Kim, H.; Hamers, R. J. Photochemical Grafting and Patterning of Biomolecular Layers onto $TiO_2$ Thin Films. *ACS Appl. Mater. Intefaces* **2009**, *1*, 1013−1022.
(42) Rosso, M.; Giesbers, M.; Arafat, A.; Schroen, K.; Zuilhof, H. Covalently Attached Organic Monolayers on SiC and $Si_xN_4$ Surfaces: Formation Using UV Light at Room Temperature. *Langmuir* **2009**, *25*, 2172−2180.
(43) Ruther, R. E.; Franking, R.; Huhn, A. M.; Gomez-Zayas, J.; Hamers, R. J. Formation of Smooth, Conformal Molecular Layers on ZnO Surfaces via Photochemical Grafting. *Langmuir* **2011**, *27*, 10604−10614.
(44) Mischki, T. K.; Donkers, R. L.; Eves, B. J.; Lopinski, G. P.; Wayner, D. D. M. Reaction of Alkenes with Hydrogen-Terminated and Photooxidized Silicon Surfaces. A Comparison of Thermal and Photochemical Processes. *Langmuir* **2006**, *22*, 8359−8365.
(45) Matienzo, L. J.; Yin, L. I.; Grim, S. O.; Swartz, W. E. X-Ray Photoelectron Spectroscopy of Nickel Compounds. *Inorg. Chem.* **1973**, *12*, 2762−2769.
(46) Bansal, A.; Li, X.; Lauermann, I.; Lewis, N. S.; Yi, S. I.; Weinberg, W. H. Alkylation of Si Surfaces Using a Two-Step Halogenation/Grignard Route. *J. Am. Chem. Soc.* **1996**, *118*, 7225−7226.
(47) O'Leary, L. E.; Johansson, E.; Brunschwig, B. S.; Lewis, N. S. Synthesis and Characterization of Mixed Methyl/Allyl Monolayers on Si(111). *J. Phys. Chem. B* **2010**, *114*, 14298−14302.
(48) Chen, Y. W.; Prange, J. D.; Dühnen, S.; Park, Y.; Gunji, M.; Chidsey, C. E. D.; McIntyre, P. D. Atomic Layer-Deposited Tunnel Oxide Stabilizes Silicon Photoanodes for Water Oxidation. *Nat. Mater.* **2011**, *10*, 539−544.
(49) Lee, M. H.; Takei, K.; Zhang, J.; Kapadia, R.; Zheng, M.; Chen, Y.-Z.; Nah, J.; Matthews, T. S.; Chueh, Y.-L.; Ager, J. W.; Javey, A. p-Type InP Nanopillar Photocathodes for Efficient Solar-Driven Hydrogen Production. *Angew. Chem., Int. Ed.* **2012**, *51*, 10760−10764.
(50) Seger, B.; Pedersen, T.; Laursen, A. B.; Vesborg, P. C. K.; Hansen, O.; Chorkendorff, I. Using $TiO_2$ as a Conductive Protective Layer for Photocathodic $H_2$ Evolution. *J. Am. Chem. Soc.* **2013**, DOI: 10.1021/ja309523t.